

pubs.acs.org/Macromolecules Article

# Controlled Synthesis of Crystalline and Helical N-Alkyl Poly(L-alanine)

Wenxiao Liu, Xuehua Deng, Yutong Dong, Sunting Xuan,\* and Zhengbiao Zhang\*



**Cite This:** *Macromolecules* 2024, 57, 7031–7042



**ACCESS** I

III Metrics & More

Article Recommendations

SI Supporting Information

**ABSTRACT:** The synthesis of N-substituted polypeptides is challenging due to steric hindrance. Here, N-alkyl poly(L-alanine)s, with controlled molecular weights ( $M_n$ s) and narrow distributions, were efficiently synthesized by primary amine-initiated and acetic acid-catalyzed ring-opening polymerizations of N-alkyl-(L)-alanine N-carboxyanhydrides [ $^N$ Alkyl-(L)-Ala-NCAs] in toluene of low polarity and low proton-accepting ability. The N-alkyl poly(L-alanine)s, with chiral centers at backbones and different alkyl substituents at side chains, showed a relatively extended helical structure similar to that of

the PPII-helix of poly(L-proline). The elongation of the alkyl side chains and the increase in temperatures had negligible effects on the helix structure, as revealed by the circular dichroism measurements. The differential scanning calorimetry and X-ray diffraction measurements showed that the polymers were crystalline. Besides, the  $^{N}$ Alkyl-(L)-Ala-NCAs were capable of copolymerizing with other monomers, producing structurally diverse copolymers. The efficient synthesis of N-alkyl poly(L-alanine)s, combined with the structural tunability, hydrophobicity, crystallinity, protein-like skeleton, enzymatic stability, and stable helix, makes the polymers attractive structural units in self-assembly and the biomedical field.

## **■ INTRODUCTION**

Polypeptides and polypeptoids, with protein-like skeleton structures, have received considerable attention due to their facile synthesis, structural tunability, and biocompatibility. <sup>1–4</sup> Polypeptides have both chiral centers and hydrogen bond donors along backbones, which are prone to crystallize and form secondary structures (e.g.,  $\alpha$ -helix and  $\beta$ -sheet) (Figure 1a). <sup>5</sup> Polypeptoids, which are structural mimics of polypeptides, have substituents at the nitrogen atoms instead of the  $\alpha$ -carbons (Figure 1b). <sup>4</sup> This simple structural change has made polypeptoids absent of both chiral centers and hydrogen bond donors along the backbones. Compared to polypeptides, polypeptoids show enhanced solubility in commonly used solvents, enzymatic stability, and thermal processability. <sup>4,6–8</sup>

N-substituted polypeptides (a.k.a disubstituted polypeptioids) combine the structural characteristics of polypeptides and polypeptoids, which have both chiral centers along the backbones and N-substituents (Figure 1c). Many naturally occurring peptide drugs, such as immunosuppressive drug cyclosporine 18 and anticancer drug actinomycin D, 9-11 have structural units of N-substituted peptide. The N-substitution has conferred them improved membrane permeability, proteolytic resistance, pharmacokinetic properties, and structural rigidity compared to peptides. N-substituted polypeptides also show enhanced protein affinity due to conformational restrictions. Apart from the natural drugs, many proteins, such as collagen and gelatin, also contain structural units of N-substituted peptide, i.e., poly(L-proline) (PLP). 13,14 L-Proline is the only N-substituted amino acid in the human

body and PLP has been shown to form helical structures though no hydrogen bond donors are present along the backbone. 15,16 The synthesis of PLP has been challenging due to poor solubility until recently Lu group reported the efficient ring-opening polymerization (ROP) of L-proline-N-carbox-yanhydride (L-pro-NCA) in the mixed solvent of acetonitrile and water. N-substituted polypeptides other than PLP, however, have been rarely reported due to the difficulty of synthesis and their properties have not been fully investigated. Therefore, it is necessary to establish efficient synthesis methods for N-substituted polypeptides, laying the foundation for structure—property investigations and application explorations.

The development toward the ROPs of amino acid-*N*-(thio)carboxyanhydrides (NCAs and NTAs) and N-substituted glycine *N*-(thio)carboxyanhydrides (NNCAs and NNTAs) have produced various polypeptides and polypeptides. Different initiators and catalysts, including ammonium hydrochloride, <sup>17,18</sup> Ni/Co-based organometallic catalysts, <sup>19</sup> rare earth catalysts, <sup>20</sup> lithium hexamethyldisilazide, <sup>21,22</sup> hexamethyldisilazane, <sup>23</sup> trimethylsilyl sulfide, <sup>24</sup> fluorinated alco-

Received: May 16, 2024 Revised: July 5, 2024 Accepted: July 9, 2024 Published: July 20, 2024





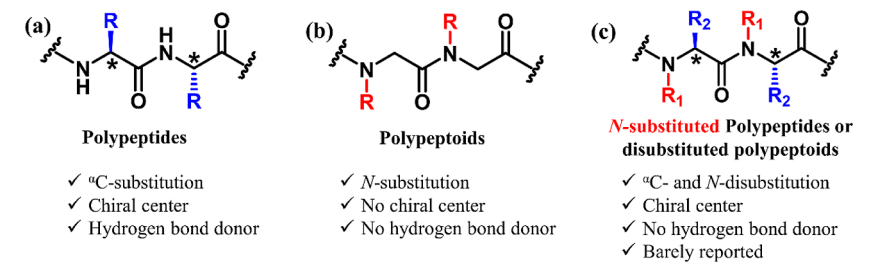
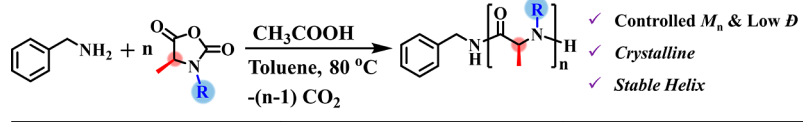


Figure 1. Chemical structures of polypeptides, polypeptoids, and N-substituted polypeptides.



R	Monomer	Polymer
28/	$^{N}$ Me-( $L$ )- $Ala$ -NCA ( $M_1$ )	L-PNMA
32/	$^{N}$ Et-( $L$ )- $Ala$ -NCA ( $M_2$ )	L-PNEA
*****	NPr-(L)-Ala-NCA (M <sub>3</sub> )	L-PNPrA
*****	<sup>N</sup> Bu-(L)-Ala-NCA (M <sub>4</sub> )	L-PNBA
3,~~~	<sup>N</sup> Pen-(L)-Ala-NCA (M <sub>5</sub> )	L-PNPenA
\\\\\\\\\\\\\\\\\\\\\\\\\\\\\\\\\\\\\\	$^{N}$ Hex-( $L$ )- $Ala$ -NCA ( $M_6$ )	L-PNHA

Figure 2. Synthesis of N-alkyl poly(L-alanine)s by benzylamine-initiated and AA-catalyzed ROPs in toluene.

hols,<sup>25</sup> urea,<sup>26</sup> crown ether,<sup>27</sup> carboxylates,<sup>28</sup> etc., have been reported to achieve the rapid and controlled ROPs of NCAs/ NTAs and NNCAs/NNTAs. In recent years, the controlled ROPs of NCAs/NTAs and NNCAs/NNTAs catalyzed by organic acids have also been reported.<sup>29–33</sup> The studies of Nsubstituted polypeptides have nevertheless been rarely reported due to the difficulty of their synthesis. The primaryinitiated ROPs and solid-phase synthesis failed to efficiently synthesize N-substituted polypeptides due to the steric hindrance added by the disubstitution. 12,34-38 Our group recently reported, for the first time, the rapid and controlled ROPs of N-methyl-α-amino acids N-carboxyanhydrides ( $\alpha$ NNCAs) using acetic acid (AA) as the catalyst and primary amine as the initiator.<sup>39</sup> The AA was shown to play multiple roles in the ROPs:<sup>32,39</sup> (1) activates the monomers via hydrogen bonding interaction; (2) facilitates nucleophilic addition-elimination by proton exchange; (3) facilitates the release of CO2; and (4) forms acid-base equilibrium at the propagation center. This method allowed us to obtain a series of N-methyl polypeptides with diverse structures, controlled molecular weights  $(M_n)$ , and narrow distributions. These Nmethyl polypeptides exhibited helical structures, high glass transition temperatures  $(T_{o}s)$ , enzymatic resistance, and low toxicity. This study, however, did not explore the synthesis and polymerization of  $\alpha$ NNCAs other than the ones with the Nmethyl substituent. The feasibility regarding the synthesis and polymerization of other  $\alpha$ NNCAs, as well as the effect of Nsubstituent on the properties of N-substituted polypeptides, has not been well investigated.

In this work, a series of *N*-alkyl-(L)-alanine-*N*-carboxyanhydrides [NAlkyl-(L)-Ala-NCAs] were successfully synthesized (Figure 2). Different initiators, catalysts, and solvents were tried for the ROPs of NAlkyl-(L)-Ala-NCAs. It was found that the polymerization was fast while controlled when using AA as the catalyst and benzylamine as the initiator in toluene, a

solvent of low polarity and low proton-accepting ability. This method produced a series of N-alkyl poly(L-alanine)s with controlled  $M_{\rm p}$ s and narrow distributions. All of the polymers exhibited an extended helix structure resembling the PPII-helix of PLP. The elongation of the alkyl side chain from methyl to hexyl barely altered the helix structure, as revealed by the circular dichroism (CD) measurements. The helix structure was also stable at elevated temperatures, which is different than the temperature-unstable helix structure of polypeptides formed by hydrogen bonding interactions. The polymers were crystalline though no hydrogen bond donors were present along the backbones, and the melting temperature was significantly affected by the length of alkyl side chains. To the best of our knowledge, this study, for the first time, efficiently synthesized N-substituted polypeptides with various N-alkyl side chains, which have previously been considered difficult to synthesize. The efficient synthesis, in combination with the stable helix structure, hydrophobicity, crystallinity, and enzymatic stability of N-alkyl polypeptides, makes the polymers desirable structural units in self-assembly and biomedical fields.

## **■ EXPERIMENTAL SECTION**

Materials. L-Glutamate-r-benzyl ester, cyclopentylamine, Boc-Lalanine, ethylene oxide, iodomethane, iodoethane, phosphorus trichloride (PCl<sub>3</sub>), 1,3,5-trimethoxybenzene, triethylamine, and trifluoroethanol (TFE) were purchased from Macklin (Beijing, China). L-Alanine, di-tert-butyl decarbonate, and anhydrous potassium carbonate were purchased from Aladdin (Shanghai, China). Sodium hydride (60% in mineral oil), sodium borohydride, and anhydrous acetonitrile were purchased from J&K (Shanghai, China). Propionaldehyde, butyraldehyde, valeraldehyde, hexaldehyde, and crown ether (18-C-6) were purchased from TCI (Shanghai, China). Anhydrous toluene, dichloromethane (DCM), and tetrahydrofuran (THF) were obtained from the solvent purification system. Anhydrous methanol, anhydrous hexane, anhydrous diethyl ether,

and ethyl acetate were purchased from Qiangsheng (Suzhou, China). Benzylamine, 1,3-bis [3,5-bis (trifluoromethyl) phenyl] urea (U–O), 1,3-bis [3,5-bis (trifluoroethyl) phenyl] thiourea (U–S), and 1,1,3,3-tetramethylguanidine (TMG) were purchased from Sigma-Aldrich (Shanghai, China). CDCl $_3$ , THF- $d_8$ , DMSO- $d_6$ , and CD $_2$ Cl $_2$  were purchased from Energy Chemical (Shanghai, China). Hydrochloric acid and AA were purchased from Yonghua (Suzhou, China). Silicon wafers were purchased from SKJYLEAN (Suzhou, China).

Instruments. Nuclear Magnetic Resonance Spectroscopy. All <sup>1</sup>H and <sup>13</sup>C nuclear magnetic resonance (NMR) spectra were recorded on a Bruker nuclear magnetic resonance instrument (300 MHz) using tetramethylsilane as the internal standard at room temperature. The <sup>1</sup>H NMR spectra were referenced to 7.26 ppm in CDCl<sub>3</sub> and 5.32 ppm in CD<sub>2</sub>Cl<sub>2</sub>. <sup>13</sup>C NMR spectra were referenced to 77.00 ppm in CDCl<sub>3</sub> and 53.84 ppm in CD<sub>2</sub>Cl<sub>2</sub>.

Matrix-Assisted Laser Desorption/Ionization Time-of-Flight Mass Spectrometry. Matrix-assisted laser desorption/ionization time-of-flight (MALDI-TOF) mass spectra were recorded on an UltrafleXtreme III MALDI-TOF mass spectrometer (Bruker Daltonics, Germany) equipped with an Nd/YAG smart beam-II laser with 355 nm wavelength and 200 Hz firing rate. The MTP 384 target plate was used for sample preparation. The instrument was calibrated with PMMA prior to each measurement. The trans-2-[3-(4tert-butylphenyl)-2-methyl-2-propenylidene]malononitrile (DCTB) and sodium trifluoroacetate (NaTFA) were used as the matrix and cationizing agent, respectively. The DCTB in CHCl<sub>3</sub> (20 mg/mL) and NaTFA in ethanol (10 mg/mL) were mixed at a 10:1 (v/v) ratio. All samples were dissolved in CHCl<sub>3</sub> at a concentration of 10 mg/mL. The sample was prepared by a "sandwich" sampling method. The mixture of DCTB and NaTFA (8  $\mu$ L) was added onto the target plate followed by addition of the sample solution (8  $\mu$ L), and then, the mixture of DCTB and NaTFA (8 µL) was added on top. After evaporation of the solvent, the target plate was inserted into a MALDI-TOF mass spectrometer. For high-resolution mass analysis, the instrument was operated in the reflector mode.

Size-Exclusion Chromatography. The number-average molecular weight  $(M_{\rm n})$  and molecular weight dispersity  $(D=M_{\rm w}/M_{\rm n})$  of the polymers were determined using the TOSOH HLC-8320 size-exclusion chromatography (SEC) system equipped with two TSKgel Super 20 Multipore HZ-N (4.6 × 150 mm, 3  $\mu$ m bead size) columns arranged in a series, automatic sampler, refractive index, and UV detectors. N,N-Dimethylformamide (DMF) containing 0.1 M LiBr was used as the eluent at a flow rate of 0.6 mL/min. The column temperature was 40 °C. The samples were dissolved in DMF with LiBr at 2 mg/mL and filtered through a 0.45  $\mu$ m PTFE syringe filter before injecting to the instrument. The  $M_{\rm n}$  and D of the polymer were determined by using polystyrene (PS) as the standard.

Circular Dichroism. The CD spectra of the polymers were recorded using a JASCO J-815 CD spectrometer equipped with a Peltier temperature control device (JASCO, Tokyo, Japan). All polymer samples were dissolved in TFE at 0.09 mg/mL and measured in square quartz cuvettes with a path length of 3 mm. Measurements were performed with a single accumulation, a bandwidth of 3 nm, and a scanning rate of 200 nm/min. For temperature-dependent measurements, the samples were heated at a rate of 10 °C/min and held at the specified temperature for 5 min prior to each measurement.

Thermogravimetric Analysis. The thermal decomposition temperatures  $(T_{\rm d}{\rm s})$  of the polymers were determined by using a TA SDT-Q600 thermogravimetric analyzer under a nitrogen atmosphere. The samples were heated from 30 to 800 °C at a heating rate of 10 °C/min

Differential Scanning Calorimetry. The thermal transitions of polymers were measured by a TA Instruments DSC 250 (New Castle, DE, USA) under a nitrogen atmosphere. The polymer sample (3  $\sim$  4 mg) was weighed in an aluminum pan (5.4  $\times$  2.6 mm, QingYi) and sealed, which was heated from 25 to 200 °C at 10 °C/min and maintained at 200 °C for 1 min before cooling to -80 °C at 10 °C/min and maintained at -80 °C for 1 min, and then was heated back to 200 °C at 10 °C/min. The second heating trace was used to

determine the glass transition temperature  $(T_{\rm g})$  and melting temperature  $(T_{\rm m})$  of the polymer.

Wide-Angle X-ray Diffraction. Wide-angle X-ray diffraction (WAXD) measurements of polymers were performed on a Bruker D8 Advance X-ray diffractometer with a Cu Kα anode ( $\lambda$  = 0.154 nm). Silicon wafers (1 × 1 cm) were immersed in a piranha solution (i.e., a mixture of  $H_2SO_4$  and  $H_2O_2$ , v/v = 7:3) for 30 min, rinsed with Milli-Q water thoroughly, and ultrasonicated in Milli-Q water for 30 min followed by rinsing with Milli-Q water. The ultrasonication and rinsing were performed 3 times, and the silicon wafers were dried in a vacuum oven at 80 °C. The polymers were placed on the above clean silicon wafer and subjected to measurement.

**Monomer Synthesis.** The monomer precursors and monomers  $(\mathbf{M_1} - \mathbf{M_6})$  were synthesized by adapting reported procedures (Schemes S1-S10). <sup>7,40,41</sup> The detailed synthetic procedures and NMR spectra are included in the Supporting Information.

Representative Procedure for AA-Promoted Polymerization. The monomer was weighed in a 5 mL vial and dissolved in toluene ([M]<sub>0</sub> = 0.4 mol/L). Upon which was added a determined amount of AA stock solution and benzylamine stock solution, respectively. The mixture was stirred at 80 °C to reach quantitative conversion, as determined by NMR spectroscopy. L-PNEA and L-PNPrA were precipitated by adding excess diethyl ether, followed by the collection of the precipitate, washing with diethyl ether, and drying under vacuum to obtain the polymer as a white solid. The L-PNBA, L-PNPenA, and L-PNHA could not be precipitated out by diethyl ether. Thus, their polymerization solutions were vacuum-dried and redissolved in DCM, followed by extraction with saturated sodium bicarbonate aqueous solution. The DCM layer was dried with anhydrous sodium sulfate and concentrated to obtain the polymer as a viscous liquid.

Representative Kinetic Studies of Benzylamine-Initiated and AA-Promoted ROPs of Monomers. The polymerization procedure was the same as that described above. 1,3,5-Trimethoxybenzene was used as an internal reference. At the designated time intervals, aliquots of the polymerization solution were drawn, and one drop of TFA was added immediately to terminate the polymerization. The solution was dried and redissolved in CDCl<sub>3</sub> for NMR analysis to determine the monomer conversion based on the integration of the internal reference and the  $\alpha$ -CH proton of the monomer. Kinetic experiments were repeated twice for each polymerization.

## ■ RESULTS AND DISCUSSION

All the monomers  $(M_1-M_6)$  were synthesized using cheap and readily available L-alanine and aldehydes in good overall yields (65-75%) by adapting reported procedures.<sup>39-41</sup> The chemical structures of all of the monomer precursors and monomers were confirmed by <sup>1</sup>H and <sup>13</sup>C NMR spectroscopy (Figures S1-S10). As mentioned above, our previous work has shown that AA as the catalyst and benzylamine as the initiator can efficiently polymerize the monomer with N-methyl side chain  $[^{N}Me-(L)-Ala-NCA, M_{1}]$  in chlorinated solvents.<sup>39</sup> Therefore, this polymerization condition was first applied to the monomer with a N-ethyl side chain [NEt-(L)-Ala-NCA,  $M_2$ ]. Unexpectedly, under the same polymerization conditions  $\{[M]_0/[I]_0/[AA]_0 = 25:1:5, 50 \, {}^{\circ}C, 1,2$ -dichloroethane (DCE)}, the polymerization rate of  $M_2$  ( $k_{obs} = 0.04 \text{ h}^{-1}$ ) was about 144 times slower than  $M_1$  ( $k_{obs} = 5.76 \text{ h}^{-1}$ ). If the methyl substituent at the  $\alpha$ -carbon was changed to ethyl [ $^{N}$ Me-( $_{L}$ )-Et-NCA,  $M_{1-2}$ ], the polymerization rate ( $k_{obs} = 0.40 \text{ h}^{-1}$ ) was about 14 times slower than that of M<sub>1</sub>. These results indicated that the increase of steric hindrance at the  $\alpha$ -carbon or nitrogen significantly slowed the polymerization of the monomer, and the polymerization rate was more affected by the N-substitution (Figure 3).

To accelerate the polymerization of  $M_2$ , recently reported initiators and catalysts (Table 1), used for the efficient ROPs of

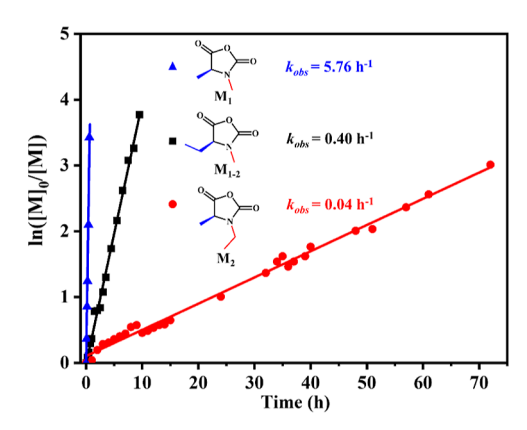


Figure 3. Polymerization kinetics of  $M_1$ ,  $M_{1-2}$ , and  $M_2$  using benzylamine as the initiator and AA as the catalyst in DCE at 50 °C ( $[M]_0/[I]_0/[AA]_0 = 25:1:5$ ).

NCAs/NTAs and NNCAs/NNTAs, were tried for the ROP of M<sub>2</sub>. Tetrabutylammonium acetate (TBAA) and TMG initiators were shown to greatly accelerate the ROPs of NCA and NNTA, respectively, through a concerted addition and decarboxylation propagation mechanism. 28,42 The primary amine-initiated ROP of NCA was significantly accelerated using crown ether (18-C-6) as the catalyst. 27 Urea (U-O) and thiourea (U-S) catalysts were shown to activate the NNCA through hydrogen bonding interaction and boost the polymerization rate.<sup>26</sup> In contrast, these initiators and catalysts failed to efficiently polymerize  $M_2$ . As shown in Table 1, when TBAA and TMG were used as initiators, the polymerizations of  $M_2$ were very slow, reaching only 3 and 11% monomer conversions, respectively, after 24 h (entries 2-3). We speculated that probably the carbamate growing centers formed in the TBAA- and TMG-initiated ROPs are not nucleophilic enough to efficiently attack the more sterically hindered disubstituted NCA (M<sub>2</sub>), resulting in slow polymerization. When U-O, U-S, or 18-C-6 was used as the catalyst

for the primary amine-initiated ROP of  $M_{2}$ , polymerization was still very slow (entries 4–7). As shown in Figure S16, the 18-C-6 can form hydrogen bonding interactions with the NH of  $\gamma$ benzyl-L-glutamate-N-carboxyanhydride (BLG-NCA), as indicated by the obvious downfield shift of the NH proton ( $\Delta \delta$  = 0.21 ppm) in the NMR spectrum of an equal molar mixture of BLG-NCA and 18-C-6 in CDCl<sub>3</sub>. The 18-C-6 served as a bridge to facilitate the close contact of the monomer and primary amine growing center, which greatly accelerated the ROP of BLG-NCA.<sup>27</sup> The M<sub>2</sub> monomer with N-substitution, however, has no NH to form hydrogen bonds with 18-C-6, and the ROP of M2 could not be catalyzed by 18-C-6. U-O and U-S have poor solubility in DCE, and thus, the polymerizations were conducted in THF. U-O and M2 were shown to form hydrogen bonds as revealed by the slight chemical shift change corresponding to the NH proton of U-O and carbonyl carbon of M2 in the equal molar mixture of U-O and M2 (Figure S17). This weak activation of  $M_2$ , however, failed to achieve the efficient ROP of the sterically hindered disubstituted  $M_2$ . In comparison, the polymerization of  $M_2$ was faster when using AA as the catalyst and benzylamine as the initiator due to the multiple roles of AA described above, which resulted in higher monomer conversions under the same polymerization condition (Tables 1 and S1). The polymerization of  $M_2$ , however, was much less efficient than that of  $M_1$ and  $M_{1-2}$  (Figure 3). When the molar ratio of  $M_2$  to initiator was increased to 50:1 and 100:1, it took 3-5 days for  $M_2$  to reach >99% conversion (Tables 1 and S1 and Figure S20).

It has been shown that solvent has a great influence on the polymerization rate of monomers. Therefore, different solvents, including DCE, toluene, DMF, and 1,2-dioxane, were tried for the ROP of  $M_2$ . The properties of solvents can be characterized by three parameters (Table S2): (1)  $\pi^*$ , an indicator of the polarity of the solvent, which measures the ability of the solvent to stabilize charges or dipoles; (2)  $\beta$ , an indicator of hydrogen bond accepting capability, measures the ability of the solvent to accept protons; and (3)  $\alpha$ , an indicator

Table 1. ROPs of M2 Using Different Initiators and Catalystsa

$NH_2$ $BnNH_2(I_1)$	$ \begin{array}{c} 0 \\ 0 \\ 0 \\ \end{array} $ $ \begin{array}{c} \end{array} $ $ \end{array} $	TMG (I <sub>3</sub> )	F F	$\begin{array}{cccccccccccccccccccccccccccccccccccc$	$\begin{array}{c} F \\ F $	F F F	18-C-6 (C <sub>3</sub> )	Д <sub>ОН</sub> АА (С <sub>4</sub> )
entry	I		C	$[M]_0/[I]_0/[$	$[C]_0$	time (h)	conv	. (%) <sup>b</sup>
1	$I_1$			25:1:0		24	1	13
2	${ m I_2}$			25:1:0		24		3
3	$I_3$			25:1:0		24		11
4 <sup>c</sup>	${\bf I_1}$		$C_1$	25:1:5		24	2	22
5 <sup>c</sup>	${\bf I_1}$		$C_2$	25:1:5		24		12
6	$I_1$		$C_3$	25:1:5		24	:	11
7	$I_1$		$C_3$	25:1:1		24		12
8	$I_1$		$C_4$	25:1:1		24	5	51
9	$I_1$		$C_4$	25:1:5		24	(	62
10	$\mathbf{I}_1$		$C_4$	50:1:10		>3 d	9	99
11	$I_1$		$C_4$	100:1:20	)	>5 d	9	99

<sup>&</sup>quot;All polymerizations were conducted at 50 °C with  $[M]_0 = 0.4 \text{ mol/L}$ . Determined by NMR spectroscopy using 1,3,5-trimethoxybenzene as the internal standard in CDCl<sub>3</sub>. All polymerizations were conducted in DCE except for entries 4–5 which were conducted in THF due to poor solubility of  $C_1$  and  $C_2$  in DCE.

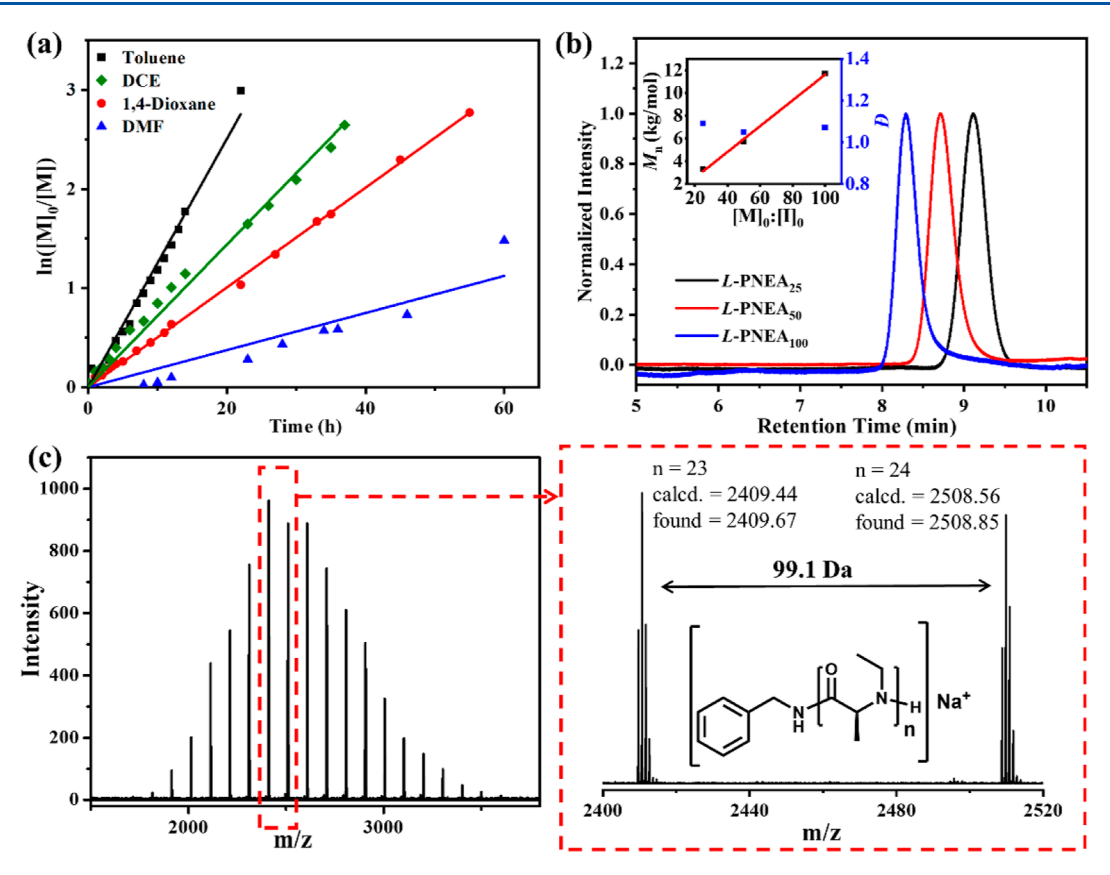


Figure 4. ROPs of  $M_2$  initiated by primary amine and catalyzed by AA: (a) polymerization kinetics of  $M_2$  in different solvents ( $[M]_0/[I]_0/[AA]_0 = 25:1:5$ ,  $[M]_0 = 0.4$  M, 50 °C); (b) SEC chromatograms of polymers synthesized by ROPs of  $M_2$  in toluene at 80 °C (Table 2, entries 5–7); and (c) MALDI-TOF mass spectrum of L-PNEA (Table 2, entry 5).

Table 2. ROPs of M<sub>2</sub> in Different Solvents<sup>a</sup>

entry	solvent	$[M]_0/[I]_0/[AA]_0$	time (h)	T (°C)	conv. (%)	$M_{\rm n'theor}^{c}$ (kg/mol)	$M_{\text{n/NMR}}^{d}$ (kg/mol)	$M_{\text{n,SEC}}^{e}(\text{kg/mol})$	$D^e$
1	DCE	25:1:5	48	50	80	1.6	2.0	1.7	1.09
2	1,4-dioxane	25:1:5	48	50	75	2.3	1.7	2.0	1.09
3	DMF	25:1:5	48	50	26	0.7			
4	toluene	25:1:5	20	50	>99	2.6	2.4	3.1	1.06
5	toluene	25:1:5	10	80	>99	2.6	2.4	3.3	1.09
6	toluene	50:1:10	36	80	>99	5.1	4.9	5.7	1.05
7	toluene	100:1:20	60	80	>99	10.0	9.8	11.7	1.07
8	toluene	200:1:40	>3 d	80	>99	19.9		19.1	1.05

<sup>&</sup>quot;All polymerizations were conducted with  $[M]_0 = 0.4 \text{ mol/L}$ . Determined by NMR spectroscopy using 1,3,5-trimethoxybenzene as the internal standard in CDCl<sub>3</sub>. Determined based on the monomer conversion and  $[M]_0/[I]_0$  ratio. Determined by end-group analysis using H NMR spectroscopy. Determined from the SEC analysis using DMF containing 0.1 M LiBr as the eluent and PS as the standard.

of the hydrogen bond donating capability, measures the ability to provide protons. As shown in Figure 4a, the polymerization rates of  $\mathbf{M}_2$  in different solvents showed the following trend:  $k_{\text{obs,toluene}}$  (0.13 h<sup>-1</sup>) >  $k_{\text{obs,DCE}}$  (0.07 h<sup>-1</sup>) >  $k_{\text{obs,1,4-dioxane}}$  (0.05 h<sup>-1</sup>) >  $k_{\text{obs,DMF}}$  (0.02 h<sup>-1</sup>). The polymerization rate was closely related to the polarity of the solvent ( $\pi^*$ ) and its ability to accept protons ( $\beta$ ). The polarity ( $\pi^*$  = 0.88) and the ability to accept protons ( $\beta$  = 0.69) of DMF are the highest among the solvents used, and the polymerization of  $\mathbf{M}_2$  in DMF was the slowest. We speculated that DMF, with a high proton-accepting ability, could form hydrogen bonds with the AA, which decreased the catalytic activity of AA and slowed down the polymerization. The high polarity and high proton-accepting ability of DMF could also enhance the solvation of the secondary amino growing chain end and decrease its

interaction with the monomer, which resulted in a slower polymerization. To support this hypothesis, the polymerization kinetics of  $\mathbf{M}_2$  without the presence of AA in the abovementioned solvents were also conducted. The polymerization was still the slowest in DMF (Figure S21), supporting the idea that the enhanced solvation of the secondary amino propagation center in DMF played an important role in the polymerization rate. In contrast, toluene exhibited a low polarity ( $\pi^*=0.54$ ) and low proton-accepting ability ( $\beta=0.11$ ), resulting in faster polymerization of  $\mathbf{M}_2$ . It should be noted that the polymerizations of  $\mathbf{M}_2$  in toluene were homogeneous, though toluene has low polarity. To further increase the polymerization rate, the temperature was increased from 50 to 80 °C. As shown in Table 2, the ROP of  $\mathbf{M}_2$  at 50 °C took 20 h to reach quantitative monomer

Table 3. ROPs of NAlkyl-(L)-Ala-NCAs Using Benzylamine as the Initiator and AA as the Catalyst in Toluene at 80 °Ca

<sup>N</sup>Pr-(L)-Ala-NCA <sup>N</sup>Bu-(L)-Ala-NCA <sup>N</sup>Pen-(L)-Ala-NCA <sup>N</sup>Hex-(L)-Ala-NCA

м

		IVI <sub>3</sub>		W1 <sub>4</sub>	N <sub>15</sub>	IVI <sub>6</sub>		
entry	monomer	$[M]_0/[I]_0/[AA]_0$	time (h)	conv. <sup>b</sup> (%)	$M_{\rm n'theor}^{c}$ (kg/mol)	$M_{\text{n},NMR}^{d}$ (kg/mol)	$M_{\text{n/SEC}}^{e}$ (kg/mol)	$D^e$
1	$\mathbf{M}_3$	25:1:5	12	>99	2.9	2.6	3.3	1.04
2	$\mathbf{M}_3$	50:1:10	40	>99	5.8	5.7	5.4	1.08
3	$\mathbf{M}_3$	100:1:20	65	>99	11.4	11.2	10.4	1.09
4	$\mathbf{M}_4$	25:1:5	16	>99	3.3	3.1	3.5	1.06
5	$\mathbf{M}_4$	50:1:10	44	>99	6.5	6.4	7.0	1.06
6	$\mathbf{M}_4$	100:1:20	70	>99	12.8	12.5	11.5	1.04
7	$\mathbf{M}_{5}$	25:1:5	20	>99	3.6	3.7	3.4	1.07
8	$M_5$	50:1:10	48	>99	7.2	6.2	6.8	1.07
9	$M_5$	100:1:20	77	>99	14.2	13.1	13.8	1.09
10	$M_6$	25:1:5	24	>99	4.0	3.7	4.2	1.07
11	$M_6$	50:1:10	50	>99	7.9	7.6	6.2	1.07
12	$\mathbf{M}_{6}$	100:1:20	85	>99	15.6	13.9	13.8	1.05

<sup>a</sup>All polymerizations were conducted with  $[M]_0 = 0.4 \text{ mol/L}$ . <sup>b</sup>Determined by NMR spectroscopy using 1,3,5-trimethoxybenzene as the internal standard in CDCl<sub>3</sub>. <sup>c</sup>Determined based on the monomer conversion and  $[M]_0/[I]_0$  ratio. <sup>d</sup>Determined by end-group analysis using <sup>1</sup>H NMR spectroscopy. <sup>e</sup>Determined from the SEC analysis using DMF containing 0.1 M LiBr as the eluent and PS as the standard.

conversion (entry 4), while only 10 h was needed at 80 °C (entry 5). Besides, the polymers obtained at 80 °C maintained controlled  $M_{\rm n}s$  and low Ds. As the  $[M]_0/[I]_0$  increased from 25:1 to 100:1, the  $M_{\rm n}s$  of the obtained polymers were linearly increased, while the distribution remained narrow (D < 1.1) (Table 2 and Figure 4b). The corresponding MALDI-TOF mass spectrum showed that the repeating unit (99.1 Da) matched the polymer structure well, and the polymer chain was exclusively end-capped with the benzylamine initiator (Figure 4c). All of the results indicated that ROPs of  $M_2$  in toluene at 80 °C showed living polymerization characteristics.

To construct polymers with different alkyl groups at the nitrogen atom, a series of N-alkyl-(L)-alanine-N-carboxyanhydrides [ $^{N}$ Alkyl-(L)-Ala-NCAs] ( $\mathbf{M_{3}}$ – $\mathbf{M_{6}}$ ) were successfully synthesized using cheap and readily available (L)-alanine and aldehydes. The monomers were polymerized using the above-established method. All of the monomers underwent efficient ROPs to produce the corresponding polymers with controlled  $M_{n}$ s and narrow distributions (Figures S27–30 and Table 3). The MALDI-TOF mass spectra also revealed that all polymers were end-capped with the benzylamine initiator (Figures S27–30).  $^{1}$ H and  $^{13}$ NMR spectra further supported the chemical structures of the polymers (Figures S22–26).

CD is commonly used to characterize the secondary structures of proteins. To investigate the effect of *N*-substitution on the secondary structures of the polymers, *N*-alkyl polyalanines were analyzed using CD. As shown in Figure 5a, *N*-alkyl polyalanines with varying side chain lengths exhibited a positive and a negative absorption band near 200 and 225 nm in TFE, respectively, in agreement with the results of the *N*-alkyl oligoalanines prepared by solid-phase synthesis. The same and the substituent length increased, a slight redshift of the bands was observed, likely due to the increased hydrophobicity. The bands was observed, likely due to the increased hydrophobicity. The bands was observed, likely due to the increased hydrophobicity. The bands was observed, likely due to the increased hydrophobicity. The bands was observed, likely due to the increased hydrophobicity. The bands was observed, likely due to the increased hydrophobicity. The bands was observed, likely due to the increased hydrophobicity. The bands was observed, likely due to the increased hydrophobicity. The bands was observed, likely due to the increased hydrophobicity. The bands was observed, likely due to the increased hydrophobicity. The bands was observed, likely due to the increased hydrophobicity. The bands was observed, likely due to the increased hydrophobicity. The bands was observed, likely due to the increased hydrophobicity. The bands was observed, likely due to the increased hydrophobicity. The bands was observed, likely due to the increased hydrophobicity. The bands was observed, likely due to the increased hydrophobicity.

PLP has a constrained ring structure connecting the backbone and side chain, while L-PNEA has separate  ${}^{\alpha}$ C- and Nsubstituents. The PLP synthesized by ROP of L-proline-NCA in DCE formed a right-handed compact helical structure (PPIhelix), showing a negative absorption band near 200 nm and a positive absorption band near 215 nm (Figure 5b).<sup>51</sup> In contrast, PLP synthesized by ROP of L-proline-NCA in the acetonitrile-water mixed solvent formed a left-handed more extended helix (PPII-helix), showing a negative absorption band near 206 nm and a very weak positive absorption band near 225 nm (Figure 5b). 16,49 The CD spectrum of L-PNEA more resembled the PPII-helix, except for the redshift of the absorption bands (Figure 5b). Also, studies have shown that N-alkyl oligoalanines prepared by solid phase synthesis have more extended chain structures, similar to the extended PPIIhelix, based on molecular dynamics simulations, single-crystal X-ray crystallography, and NMR spectroscopy. 38,49 PPI-helix could gradually transform to the PPII-helix with increasing temperatures (Figure 5c). The CD signals of L-PNEA (structurally similar to PLP), however, did not change significantly with the increase of temperatures, indicating the stability of the helical structure (Figure 5d). The transformation between the PPI-helix and PPII-helix found in PLP was not observed in its structurally similar L-PNEA. It should also be noted that the N-alkyl polyalanines exhibited similar CD signals in other solvents such as methanol (Figure S38).

According to the reported studies, N-methyl polyglycine and N-ethyl polyglycine (PNMG and PNEG), respectively, are amorphous (Figure 6a). With the increase in N-alkyl length, the polypeptoids showed crystallinity (Figure 6a). Compared to polypeptoids, N-alkyl polyalanines have an additional methyl group at the  $\alpha$ -carbon, resulting in chiral centers along the backbone. To investigate the thermal and crystallization behaviors of N-alkyl-polyalanines, thermogravimetric analysis (TGA), differential scanning calorimetry (DSC), and X-ray diffraction were performed. TGA showed that the decomposition temperature ( $T_{\rm d}$ ) of L-PNEA was over

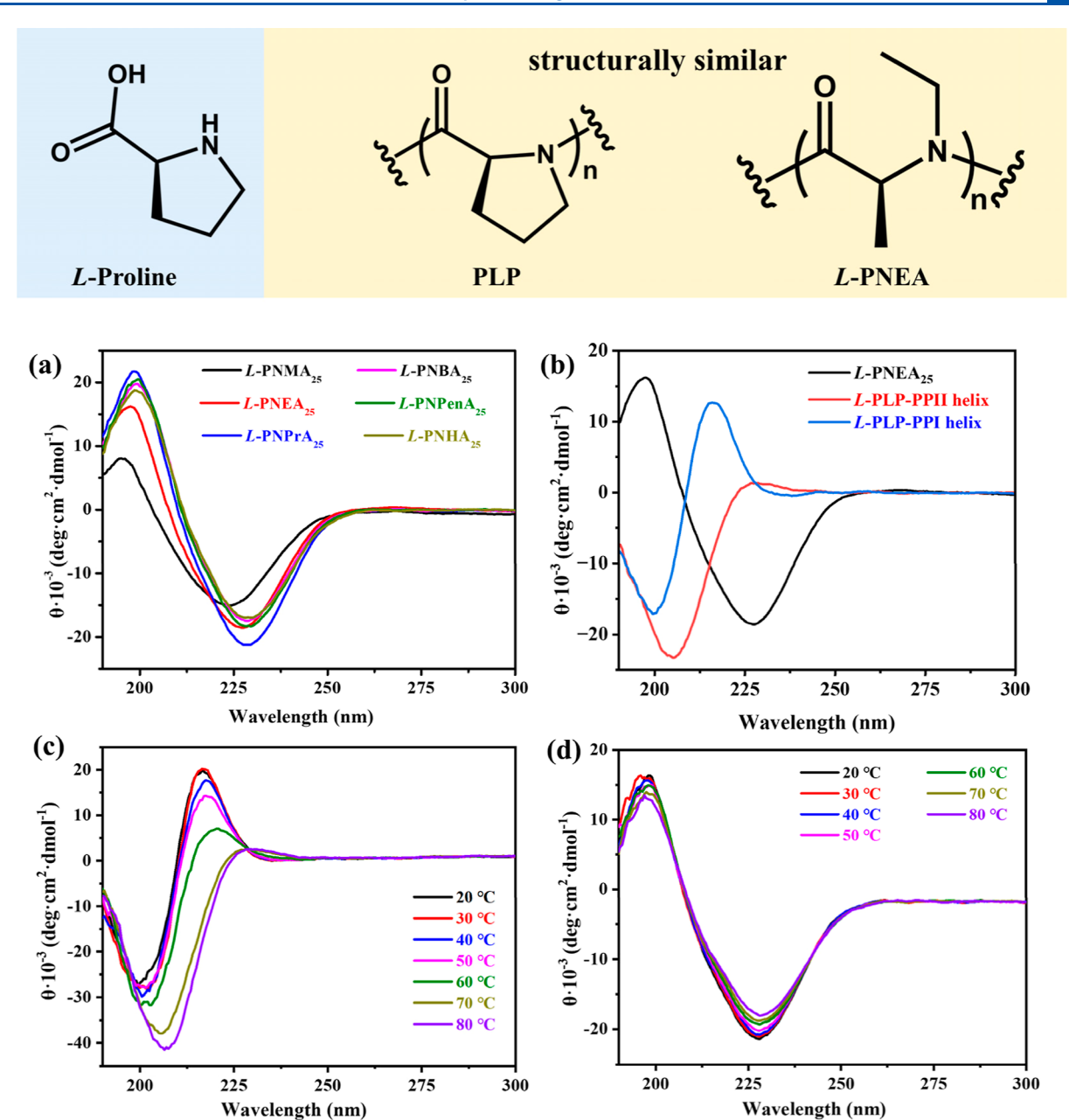


Figure 5. CD spectra of N-alkyl-poly(L-alanine)s and PLP in TFE: (a) CD spectra of N-alkyl-poly(L-alanine)s; (b) CD spectra of L-PNEA<sub>25</sub>, PLP of PPI-helix, and PLP of PPII-helix; (c) CD spectra of PPI-helix with increasing temperatures; and (d) CD spectra of L-PNEA<sub>25</sub> with increasing temperatures.

300 °C (Figure 6b). DSC analysis (Figure 6c) revealed no significant endothermic peaks for polymers with N-substituents of methyl, ethyl, and propyl below 250 °C. The polymers turned to yellow solids by heating above the  $T_d$ , indicating that the melting temperatures  $(T_{\rm m}s)$  were above the  $T_{\rm d}$ . Crystallization peaks were clearly observed in WAXD measurements (Figure 6d), suggesting the crystalline feature of the polymers, although no strong hydrogen bonding interactions were present between chains. The crystalline Nmethyl and N-ethyl poly(L-alanines) with high  $T_{\rm m}$  were in sharp contrast to the amorphous PNMG and PNEG. This is probably due to the chiral centers along the backbones of L-PNMA and L-PNEA, which increase the chain rigidity and promote packing of the polymer chains. As the N-alkyl length increased to butyl (L-PNBA), the  $T_{\rm m}$  of the polymer decreased and exhibited a melting transition in the DSC thermogram ( $T_{\rm m}$ 

= 162.5 °C). As the N-alkyl length further increased to pentyl and hexyl (L-PNPenA and L-PNHA), the polymers transitioned from solid to viscous liquids, displaying only glass transition temperatures in the DSC heating traces. These results suggested that the  $T_{\rm m}$  and crystallinity of N-alkyl-polypeptides decreased as the N-alkyl length increased, which was different from the case for the polypeptoids. The WAXD analysis of L-PNPenA and L-PNHA displayed no noticeable sharp peaks (Figure S39), further corroborating that these polymers are not crystalline.

To demonstrate the feasibility of structural diversification, proof-of-concept copolymerizations of  $\mathbf{M}_2$  with other monomers were attempted. Here, BLG-NCA, one of the most reported NCAs, was chosen as a typical NCA for the copolymerizations. The bulky N-cyclopentyl-glycine-N-carboxyanhydride ( $^{\text{Cp}}N$ -Gly-NCA) was chosen as the NNCA

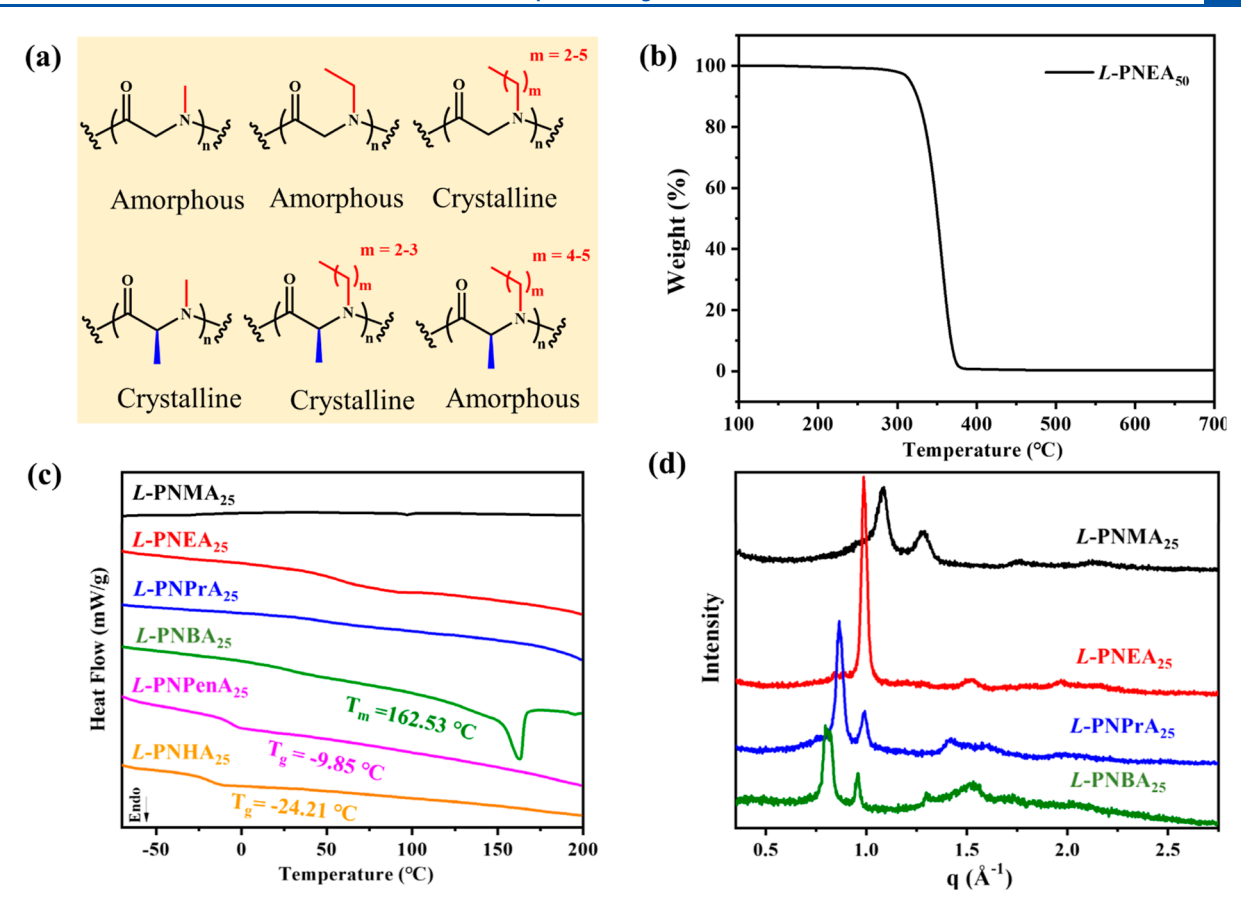


Figure 6. (a) Structures of N-alkyl polyglycines and N-alkyl poly(L-alanine)s; (b) TGA thermogram of L-PNEA<sub>50</sub>; (c) DSC thermograms of N-alkyl poly(L-alanine)s; and (d) WAXD characterization of N-alkyl poly(L-alanine)s.

monomer for the copolymerizations. The previously mentioned U-O, U-S, and 18-C-6 are not ideal catalysts for the copolymerizations, as they failed to efficiently polymerize  $M_2$ (Table 1). The AA, however, is a universal catalyst for NCAs, NNCAs, and N-alkyl-(L)-Ala-NCAs. Fast while controlled ROPs were achieved for the BLG-NCA and CpN-Gly-NCA using primary amine as the initiator and AA as the catalyst (Figure S33 and Table S3). Therefore, primary amine-initiated and AA-catalyzed block copolymerizations of M2 with BLG-NCA and <sup>Cp</sup>N-Gly-NCA were conducted. As shown in Table S3, the BLG-NCA was first polymerized at 25 °C to reach quantitative conversion, upon which the second monomer  $(^{Cp}N$ -Gly-NCA or  $M_2)$  was added, and the temperature was increased to 50 °C to accelerate the polymerization. Nearly no conversion for the second monomer, however, was observed. The MALDI-TOF spectrum of the solution revealed a cyclic amide end group (Figure S34), indicating that the primary amine growing end attacked the benzyl ester side chain at 50 °C to form the cyclic amide and terminate the polymerization. When M<sub>2</sub> was first polymerized at 50 °C and BLG-NCA was added as the second monomer at 25 °C, quantitative monomer conversion was reached to obtain block copolymer L-PNEA-b-PBLG (Table S4). The block copolymerizations of  $M_2$  with <sup>Cp</sup>N-Gly-NCA were also successfully conducted, producing block copolymers with controlled  $M_n$ s and narrow distributions (Table S3 and Figure 7a). The MALDI-TOF MS spectrum of PNEA-b-PNCpG indicated that the copolymer was endcapped with benzylamine, confirming the end group integrity of the copolymer (Figure S40). The diffusion-ordered NMR spectroscopy (1H DOSY) further proved the successful

synthesis of the block copolymer (Figure S35). The  $\mathbf{M_4}$  was also successfully copolymerized with the common N-methylglycine-N-carboxyanhydride (MeN-Gly-NCA) to produce the amphiphilic block copolymer (Figure S36). One-pot copolymerizations of CPN-Gly-NCA and  $\mathbf{M_2}$  at different monomer molar ratios produced copolymers of different compositions. The copolymers showed  $M_n$ s comparable  $M_n$ s to the theoretical values and narrow distributions (Table S5 and Figure 7b).

The L-PNEA is an ideal structural unit to confer copolymers helicity. The block copolymer L-PNEA-b-PNCpG displayed CD signals which were nearly unchanged with increasing temperatures, suggesting the stable helical structure (Figure S37). For the one-pot copolymerized L-PNEA-co-PNCpG, the helicity could be controlled by tuning the composition of L-PNEA. As shown in Figure 7c, when the total chain length was kept the same, the helicity of the copolymer was gradually increased as the content of L-PNEA was increased. The helical structure remained stable as the temperature increased from 20 to 80 °C (Figure 7d). These results suggested that <sup>N</sup>Alkyl-(L)-Ala-NCA is an ideal copolymerizable monomer, capable of conferring copolymer helicity and hydrophobicity.

## CONCLUSIONS

In this study, N-alkyl poly(L-alanines), which are challenging to synthesize, were efficiently synthesized by ROPs of N-alkyl-(L)-Ala-NCAs using benzylamine as the initiator and AA as the catalyst. The solvent was found to play an important role in the polymerizations. Toluene, a solvent with low polarity and low proton-accepting ability, was the best solvent screened,

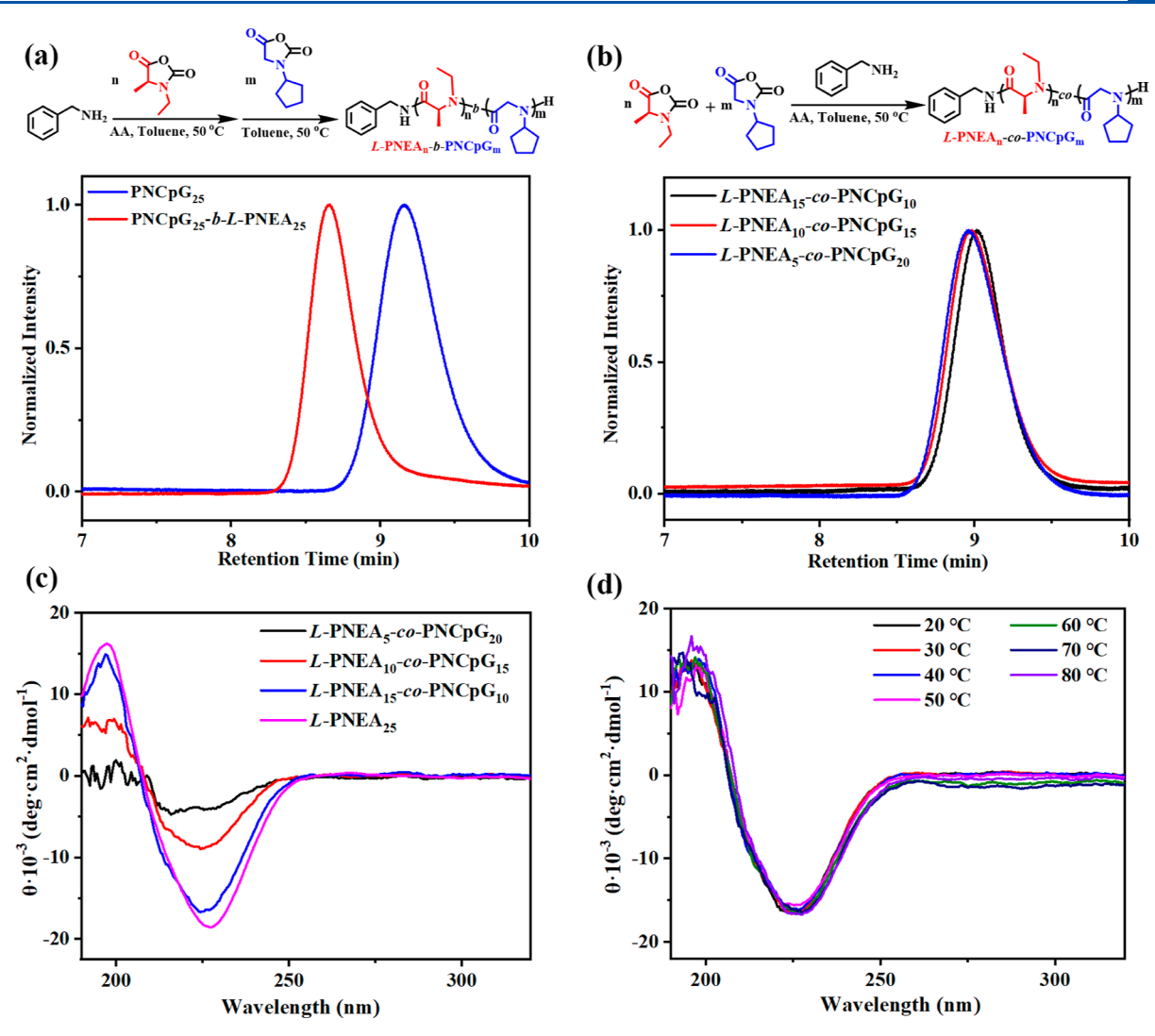


**Figure 7.** Copolymerizations of  $M_2$  and  $^{Cp}N$ -Gly-NCA: (a) synthetic procedure and SEC chromatogram of PNCpG-b-L-PNEA; (b) synthetic procedure and SEC chromatograms of L-PNEA<sub>n</sub>-co-PNCpG<sub>m</sub>; (c) CD spectra of L-PNEA<sub>n</sub>-co-PNCpG<sub>m</sub> with different composition ratios of L-PNEA; and (d) CD spectra of L-PNEA<sub>15</sub>-co-PNCpG<sub>10</sub> with increasing temperatures.

producing a series of N-alkyl poly(L-alanines) with backbone chirality, various alkyl side chains, controlled M<sub>n</sub>s and narrow distributions. The N-alkyl poly(L-alanines) showed extended helical structures, resembling the PPII-helix, which were nearly unaffected by the N-alkyl side chain length and temperature. The thermal properties and crystallization behavior of the polymers, however, were greatly affected by the length of the N-alkyl side chains. The melting temperature and crystallinity were decreased as the N-alkyl side chain length increased, which was different than that of polypeptoids showing increased crystallinity with the increase of N-alkyl length. The crystal structure will be further elucidated by more X-ray studies and molecular dynamics simulations. Besides, N-alkyl-(L)-Ala-NCAs were capable of copolymerizing with other monomers (NCAs and NNCAs) to produce diverse copolymers, greatly enriching the library of bioinspired polymers. Moreover, the N-alkyl poly(L-alanines) are ideal structural units to confer copolymers helicity and hydrophobicity. The facile synthesis, structural tunability, stable helix, crystallinity, hydrophobicity, and enzymatic stability of N-alkyl poly(L-alanines) make the polymers an attractive new generation of bioinspired material which should have potential

in self-assembly and biomedical applications (such as cryoprotectant, gene-delivery, and antibacterial materials).

## ASSOCIATED CONTENT

#### Supporting Information

The Supporting Information is available free of charge at https://pubs.acs.org/doi/10.1021/acs.macromol.4c01121.

Synthesis of <sup>N</sup>Alkyl-(L)-Ala-NCAs and N-alkyl polypeptides; <sup>1</sup>H NMR and <sup>13</sup>C NMR spectra of monomers and N-alkyl polypeptides; synthesis and characterization of  $\mathbf{M}_7$ – $\mathbf{M}_9$  and TBAA; <sup>1</sup>H NMR spectra of BLG-NCA, 18-C-6, and the equal molar mixture of BLG-NCA and 18-C-6; <sup>1</sup>H and <sup>13</sup>C NMR spectra of  $\mathbf{M}_2$ , U–O, and the equal molar mixture of  $\mathbf{M}_2$  and U–O; NMR spectra of the polymerization solution of  $\mathbf{M}_2$  at different time points; MALDI-TOF mass spectrum of L-PNEA<sub>25</sub>; SEC chromatograms of L-PNEAs using DMF (0.1 M LiBr) as the eluent; polymerization kinetics of  $\mathbf{M}_2$  in different solvents using benzylamine as the initiator in DCE at 50 °C ([ $\mathbf{M}_3$ ]0/[ $\mathbf{I}_3$ ]0 = 10:1, [ $\mathbf{M}_3$ ]0 = 0.4 mol/L); SEC chromatograms and MALDI-TOF mass spectra of N-alkyl polypeptides; synthesis of PLP in different solvents;

NMR spectra of the polymerization solution of  $M_7$  at different time points; ROPs of  $M_8$  and  $M_9$ ; polymerization kinetics of  $M_9$  catalyzed by different catalysts (U–O and AA); SEC chromatograms of L-PNCpGs; MALDI-TOF mass spectrum of L-PNCpG<sub>25</sub>; block copolymerizations of different monomers; one-pot copolymerizations of  $M_2$  and  $M_9$ ; <sup>1</sup>H DOSY spectrum of L-PNEA<sub>n</sub>-b-PNCpG<sub>m</sub>; SEC chromatograms of L-PNBA<sub>n</sub>-b-PNMG<sub>m</sub>; and CD spectra of L-PNEA<sub>25</sub>-b-PNCpG<sub>25</sub> with increasing temperatures (PDF)

#### AUTHOR INFORMATION

#### **Corresponding Authors**

Sunting Xuan — State and Local Joint Engineering Laboratory for Novel Functional Polymeric Materials, Jiangsu Key Laboratory of Advanced Functional Polymer Design and Application, Suzhou Key Laboratory of Macromolecular Design and Precision Synthesis, College of Chemistry, Chemical Engineering and Materials Science, Soochow University, Suzhou 215123, China; orcid.org/0000-0001-6499-9122; Email: stxuan@suda.edu.cn

Zhengbiao Zhang — State and Local Joint Engineering
Laboratory for Novel Functional Polymeric Materials, Jiangsu
Key Laboratory of Advanced Functional Polymer Design and
Application, Suzhou Key Laboratory of Macromolecular
Design and Precision Synthesis, College of Chemistry,
Chemical Engineering and Materials Science, Soochow
University, Suzhou 215123, China; State Key Laboratory of
Radiation Medicine and Protection, Soochow University,
Suzhou 215123, China; orcid.org/0000-0002-08298994; Email: zhangzhengbiao@suda.edu.cn

## Authors

Wenxiao Liu — State and Local Joint Engineering Laboratory for Novel Functional Polymeric Materials, Jiangsu Key Laboratory of Advanced Functional Polymer Design and Application, Suzhou Key Laboratory of Macromolecular Design and Precision Synthesis, College of Chemistry, Chemical Engineering and Materials Science, Soochow University, Suzhou 215123, China

Xuehua Deng — State and Local Joint Engineering Laboratory for Novel Functional Polymeric Materials, Jiangsu Key Laboratory of Advanced Functional Polymer Design and Application, Suzhou Key Laboratory of Macromolecular Design and Precision Synthesis, College of Chemistry, Chemical Engineering and Materials Science, Soochow University, Suzhou 215123, China

Yutong Dong — State and Local Joint Engineering Laboratory for Novel Functional Polymeric Materials, Jiangsu Key Laboratory of Advanced Functional Polymer Design and Application, Suzhou Key Laboratory of Macromolecular Design and Precision Synthesis, College of Chemistry, Chemical Engineering and Materials Science, Soochow University, Suzhou 215123, China

Complete contact information is available at: https://pubs.acs.org/10.1021/acs.macromol.4c01121

#### **Author Contributions**

S.X. and Z.Z. designed the project. W.L., X.D., and Y.D. carried out all the experiments. W.L. and S.X. wrote the manuscript.

#### Notes

The authors declare no competing financial interest.

### ACKNOWLEDGMENTS

This work was supported by the National Natural Science Foundation of China (nos. 22201197 and 21925107), the Natural Science Foundation of Jiangsu Province (BK20220507), the Collaborative Innovation Center of Suzhou Nano Science and Technology, and the National Key R&D Program of China (2022YFB3704900).

#### REFERENCES

- (1) Cai, C. H.; Lin, J. P.; Lu, Y. Q.; Zhang, Q.; Wang, L. Q. Polypeptide Self-Assemblies: Nanostructures and Bioapplications. *Chem. Soc. Rev.* **2016**, *45*, 5985–6012.
- (2) Song, Z. Y.; Han, Z. Y.; Lv, S. X.; Chen, C. Y.; Chen, L.; Yin, L. C.; Cheng, J. J. Synthetic Polypeptides: from Polymer Design to Supramolecular Assembly and Biomedical Application. *Chem. Soc. Rev.* **2017**, *46*, 6570–6599.
- (3) Xuan, S. T.; Zuckermann, R. N. Diblock Copolypeptoids: A Review of Phase Separation, Crystallization, Self-assembly and Biological Applications. *J. Mater. Chem. B* **2020**, *8*, 5380–5394.
- (4) Chan, B. A.; Xuan, S.; Li, A.; Simpson, J. M.; Sternhagen, G. L.; Yu, T.; Darvish, O. A.; Jiang, N.; Zhang, D. Polypeptoid Polymers: Synthesis, Characterization, and Properties. *Biopolymers* **2018**, *109*, No. e23070.
- (5) Song, Z. Y.; Fu, H. L.; Wang, R.; Pacheco, L. A.; Wang, X.; Lin, Y.; Cheng, J. J. Secondary Structures in Synthetic Polypeptides from *N*-Carboxyanhydrides: Design, Modulation, Association, and Material Applications. *Chem. Soc. Rev.* **2018**, *47*, 7401–7425.
- (6) Lee, C. U.; Li, A.; Ghale, K.; Zhang, D. H. Crystallization and Melting Behaviors of Cyclic and Linear Polypeptoids with Alkyl Side Chains. *Macromolecules* **2013**, *46*, 8213–8223.
- (7) Xuan, S. T.; Gupta, S.; Li, X.; Bleuel, M.; Schneider, G. J.; Zhang, D. H. Synthesis and Characterization of Well-Defined PEGylated Polypeptoids as Protein-Resistant Polymers. *Biomacromolecules* **2017**, *18*, 951–964.
- (8) Miller, S. M.; Simon, R. J.; Ng, S.; Zuckermann, R. N.; Kerr, J. M.; Moos, W. H. Proteolytic Studies of Homologous Peptide and N-Substituted Glycine Peptoid Oligomers. *Bioorg. Med. Chem. Lett.* **1994**, *4*, 2657–2662.
- (9) Wenger, R. M. Synthesis of Cyclosporine and Analogues: Structural Requirements for Immunosuppressive Activity. *Angew. Chem., Int. Ed.* **1985**, 24, 77–85.
- (10) Chatterjee, J.; Gilon, C.; Hoffman, A.; Kessler, H. N-Methylation of Peptides: A New Perspective in Medicinal Chemistry. *Acc. Chem. Res.* **2008**, *41*, 1331–1342.
- (11) Avendaño, C.; Carlos Menéndez, J. Anticancer Drugs Acting via Radical Species, Photosensitizers and Photodynamic Therapy of Cancer. In *Medicinal Chemistry of Anticancer Drugs*; Elsevier, 2008; pp 93–138
- (12) Gao, Y.; Kodadek, T. Synthesis and Screening of Stereochemically Diverse Combinatorial Libraries of Peptide Tertiary Amides. *Chem. Biol.* **2013**, *20*, 360–369.
- (13) Shoulders, M. D.; Raines, R. T. Collagen Structure and Stability. *Annu. Rev. Biochem.* **2009**, *78*, 929–958.
- (14) Jenness, D. D.; Sprecher, C.; Johnson, W. C. Circular Dichroism of Collagen, Gelatin, and Poly(proline) II in the Vacuum Ultraviolet. *Biopolymers* **1976**, *15*, 513–521.
- (15) Judge, N.; Georgiou, P. G.; Bissoyi, A.; Ahmad, A.; Heise, A.; Gibson, M. I. High Molecular Weight Polyproline as a Potential Biosourced Ice Growth Inhibitor: Synthesis, Ice Recrystallization Inhibition, and Specific Ice Face Binding. *Biomacromolecules* **2023**, 24, 2459–2468.
- (16) Hu, Y.; Tian, Z.-Y.; Xiong, W.; Wang, D.; Zhao, R.; Xie, Y.; Song, Y.-Q.; Zhu, J.; Lu, H. Water-assisted and protein-initiated fast and controlled ring-opening polymerization of proline *N*-carbox-yanhydride. *Natl. Sci. Rev.* **2022**, *9*, nwac033.
- (17) Conejos-Sánchez, I.; Duro-Castano, A.; Birke, A.; Barz, M.; Vicent, M. J. A Controlled and Versatile NCA Polymerization Method for the Synthesis of Polypeptides. *Polym. Chem.* **2013**, *4*, 3182–3186.

- (18) Vacogne, C. D.; Schlaad, H. Primary Ammonium/tertiary Amine-Mediated Controlled Ring Opening Polymerisation of Amino Acid N-Carboxyanhydrides. Chem. Commun. 2015, 51, 15645—15648.
- (19) Deming, T. J. Facile Synthesis of Block Copolypeptides of Defined Architecture. *Nature* **1997**, *390*, 386–389.
- (20) Peng, H.; Ling, J.; Shen, Z. Ring opening polymerization of  $\alpha$ -amino acid N-carboxyanhydrides catalyzed by rare earth catalysts: Polymerization characteristics and mechanism. *J. Polym. Sci., Part A: Polym. Chem.* **2012**, *50*, 1076–1085.
- (21) Wu, Y.; Zhang, D.; Ma, P.; Zhou, R.; Hua, L.; Liu, R. Lithium Hexamethyldisilazide Initiated Superfast Ring Opening Polymerization of Alpha-Amino Acid N-Carboxyanhydrides. Nat. Commun. 2018. 9, 5297.
- (22) Wu, Y.; Zhou, M.; Chen, K.; Chen, S.; Xiao, X.; Ji, Z.; Zou, J.; Liu, R. Alkali-Metal Hexamethyldisilazide Initiated Polymerization on Alpha-Amino Acid N-Substituted N-Carboxyanhydrides for Facile Polypeptoid Synthesis. *Chin. Chem. Lett.* **2021**, 32, 1675–1678.
- (23) Lu, H.; Cheng, J. J. Hexamethyldisilazane-Mediated Controlled Polymerization of  $\alpha$ -Amino Acid N-Carboxyanhydrides. *J. Am. Chem. Soc.* **2007**, *129*, 14114–14115.
- (24) Yuan, J. S.; Sun, Y. L.; Wang, J. Y.; Lu, H. Phenyl Trimethylsilyl Sulfide-Mediated Controlled Ring-Opening Polymerization of  $\alpha$ -Amino Acid N-Carboxyanhydrides. *Biomacromolecules* **2016**, *17*, 891–896.
- (25) Zhao, W.; Lv, Y.; Li, J.; Feng, Z.; Ni, Y.; Hadjichristidis, N. Fast and Selective Organocatalytic Ring-Opening Polymerization by Fluorinated Alcohol without a Cocatalyst. *Nat. Commun.* **2019**, *10*, 3590
- (26) Chen, K.; Wu, Y.; Wu, X.; Zhou, M.; Zhou, R.; Wang, J.; Xiao, X.; Yuan, Y.; Liu, R. Facile synthesis of polypeptoids bearing bulky sidechains *via* urea accelerated ring-opening polymerization of α-amino acid N-substituted N-carboxyanhydrides. *Polym. Chem.* **2022**, 13, 420–426.
- (27) Xia, Y.; Song, Z.; Tan, Z.; Xue, T.; Wei, S.; Zhu, L.; Yang, Y.; Fu, H.; Jiang, Y.; Lin, Y.; et al. Accelerated Polymerization of *N*-Carboxyanhydrides Catalyzed by Crown Ether. *Nat. Commun.* **2021**, 12, 732.
- (28) Wu, Y. M.; Chen, K.; Wu, X.; Liu, L. Q.; Zhang, W. W.; Ding, Y.; Liu, S. Q.; Zhou, M.; Shao, N.; Ji, Z. M.; et al. Superfast and Water-Insensitive Polymerization on  $\alpha$ -Amino Acid N-Carboxyanhydrides to Prepare Polypeptides Using Tetraalkylammonium Carboxylate as the Initiator. *Angew. Chem., Int. Ed.* **2021**, *60*, 26063–26071.
- (29) Siefker, D.; Williams, A. Z.; Stanley, G. G.; Zhang, D. H. Organic Acid Promoted Controlled Ring-Opening Polymerization of  $\alpha$ -Amino Acid-Derived N-thiocarboxyanhydrides (NTAs) toward Well-defined Polypeptides. ACS Macro Lett. **2018**, 7, 1272–1277.
- (30) Zheng, B. T.; Xu, S. Y.; Ni, X. F.; Ling, J. Understanding Acid-Promoted Polymerization of the N-Substituted Glycine N-Thiocarboxyanhydride in Polar Solvents. *Biomacromolecules* **2021**, 22, 1579—1589.
- (31) Wang, S.; Lu, H. Ring-Opening Polymerization of Amino Acid *N*-Carboxyanhydrides with Unprotected/Reactive Side Groups. I. D-Penicillamine *N*-Carboxyanhydride. *ACS Macro Lett.* **2023**, *12*, 555–562.
- (32) Wang, S.; Lu, M. Y.; Wan, S. K.; Lyu, C. Y.; Tian, Z. Y.; Liu, K.; Lu, H. Precision Synthesis of Polysarcosine via Controlled Ring-Opening Polymerization of *N*-Carboxyanhydride: Fast Kinetics, Ultrahigh Molecular Weight, and Mechanistic Insights. *J. Am. Chem. Soc.* 2024, 146, 5678–5692.
- (33) Liu, X.; Huang, J.; Wang, J.; Sheng, H.; Yuan, Z.; Wang, W.; Li, W.; Song, Z.; Cheng, J. Accelerated and Controlled Polymerization of *N*-Carboxyanhydrides Assisted by Acids. *CCS Chem.* **2024**, 1–28.
- (34) Goodman, M.; Fried, M. Conformational Aspects of Polypeptide Structure. XX. Helical Poly-N-methyl-L-alanine. Experimental Results. I. Am. Chem. Soc. 1967, 89, 1264–1267.
- (35) Muhl, C.; Zengerling, L.; Groß, J.; Eckhardt, P.; Opatz, T.; Besenius, P.; Barz, M. Insight into the Synthesis of *N*-Methylated Polypeptides. *Polym. Chem.* **2020**, *11*, 6919–6927.

- (36) Shiraki, Y.; Yamada, S.; Endo, T. Convenient Synthetic Approach to Poly(*N*-Methyl L-alanine) Through Polycondensation of Activated Urethane Derivative of *N*-Methyl L-Alanine. *J. Polym. Sci., Part A: Polym. Chem.* **2017**, *55*, 1674–1679.
- (37) Morimoto, J.; Fukuda, Y.; Kuroda, D.; Watanabe, T.; Yoshida, F.; Asada, M.; Nakamura, T.; Senoo, A.; Nagatoishi, S.; Tsumoto, K.; et al. A Peptoid with Extended Shape in Water. *J. Am. Chem. Soc.* **2019**, *141*, 14612–14623.
- (38) Yokomine, M.; Morimoto, J.; Fukuda, Y.; Shiratori, Y.; Kuroda, D.; Ueda, T.; Takeuchi, K.; Tsumoto, K.; Sando, S. Oligo(*N*-methylalanine) as a Peptide-Based Molecular Scaffold with a Minimal Structure and High Density of Functionalizable Sites. *Angew. Chem., Int. Ed.* **2022**, *61*, No. e202200119.
- (39) Yu, X. Y.; Wang, Y.; Dong, Y. T.; Zhao, N.; Zhang, L. F.; Xuan, S. T.; Zhang, Z. B. Efficient Synthesis of N-Methyl Polypeptides by Organic Acid Promoted Controlled Ring-Opening Polymerization of N-Methyl-α-Amino Acids N-Carboxyanhydrides. *Macromolecules* **2023**, *56*, 8899–8911.
- (40) Guo, L.; Zhang, D. H. Cyclic Poly( $\alpha$ -peptoid)s and Their Block Copolymers from *N*-Heterocyclic Carbene-Mediated Ring-Opening Polymerizations of N-Substituted *N*-Carboxylanhydrides. *J. Am. Chem. Soc.* **2009**, *131*, 18072–18074.
- (41) Kaminker, R.; Kaminker, I.; Gutekunst, W. R.; Luo, Y.; Lee, S.; Niu, J.; Han, S.; Hawker, C. J. Tuning Conformation and Properties of Peptidomimetic Backbones through Dual N/C $\alpha$ -Substitution. *Chem. Commun.* **2018**, *54*, *5237*–*5240*.
- (42) Siefker, D.; Chan, B. A.; Zhang, M.; Nho, J. W.; Zhang, D. H. 1,1,3,3-Tetramethylguanidine-Mediated Zwitterionic Ring-Opening Polymerization of Sarcosine-Derived *N*-Thiocarboxyanhydride toward Well-Defined Polysarcosine. *Macromolecules* **2022**, *55*, 2509–2516.
- (43) Song, Z.; Fu, H.; Baumgartner, R.; Zhu, L.; Shih, K.-C.; Xia, Y.; Zheng, X.; Yin, L.; Chipot, C.; Lin, Y.; et al. Enzyme-Mimetic Self-Catalyzed Polymerization of Polypeptide Helices. *Nat. Commun.* **2019**, *10*, 5470.
- (44) Chen, C. Y.; Fu, H. L.; Baumgartner, R.; Song, Z. Y.; Lin, Y.; Cheng, J. J. Proximity-Induced Cooperative Polymerization in "Hinged" Helical Polypeptides. *J. Am. Chem. Soc.* **2019**, *141*, 8680–8683.
- (45) Baumgartner, R.; Fu, H.; Song, Z.; Lin, Y.; Cheng, J. Cooperative polymerization of  $\alpha$ -helices induced by macromolecular architecture. *Nat. Chem.* **2017**, *9*, 614–622.
- (46) Wang, X. F.; Song, Z. Y.; Tan, Z. Z.; Zhu, L. Y.; Xue, T. R.; Lv, S. X.; Fu, Z. H.; Zheng, X. T.; Ren, J.; Cheng, J. J. Facile Synthesis of Helical Multiblock Copolypeptides: Minimal Side Reactions with Accelerated Polymerization of *N*-Carboxyanhydrides. *ACS Macro Lett.* **2019**, *8*, 1517–1521.
- (47) Ma, A. Y.; Wang, X.; Xuan, S. T.; Zhang, Z. B. Accelerated heterogenous ring-opening polymerization towards well-defined helical poly(*N*-allyl alanine) with clickable side chains. *Sci. China: Chem.* **2024**, *67*, 2056–2062.
- (48) Kamlet, M. J.; Abboud, J. L. M.; Abraham, M. H.; Taft, R. W. Linear Solvation Energy Relationships. 23. A Comprehensive Collection of the Solvatochromic Parameters, Pi.\*, Alpha., and Beta., and Some Methods for Simplifying the Generalized Solvatochromic Equation. *J. Org. Chem.* 1983, 48, 2877–2887.
- (49) Kubyshkin, V.; Grage, S. L.; Bürck, J.; Ulrich, A. S.; Budisa, N. Transmembrane Polyproline Helix. *J. Phys. Chem. Lett.* **2018**, *9*, 2170–2174.
- (50) Shiga, S.; Yamanaka, M.; Fujiwara, W.; Hirota, S.; Goda, S.; Makabe, K. Domain-Swapping Design by Polyproline Rod Insertion. *Chembiochem* **2019**, 20, 2454–2457.
- (51) Kakinoki, S.; Hirano, Y.; Oka, M. On the Stability of Polyproline-I and II Structures of Proline Oligopeptides. *Polym. Bull.* **2005**, *S3*, 109–115.

# ■ NOTE ADDED AFTER ASAP PUBLICATION

This paper was published ASAP on July 20, 2024 with an error in the Abstract/Table of Contents graphic. The corrected version was reposted on July 22, 2024.